ИНСТИТУТ ЯДЕРНОЙ ФИЗИКИ СО АН СССР

V.N. Baier, V.M. Katkov and V.M. Strakhovenko

CASCADE PROCESSES IN THE FIELDS OF THE AXES OF ALIGNED SINGLE CRYSTALS

PREPRINT 86-128

НОВОСИБИРСК
1986

CASCADE PROCESSES IN THE FIELDS OF THE AXES OF ALIGNED SINGLE CRYSTALS

V.N.Baier, V.M.Katkov and V.M.Strakhovenko

Institute of Nuclear Physics, 630090 Novosibirsk, USSR

A b s t r a c t

A theory is developed of electron-photon showers occurring in the fields of the axes of aligned single crystals. At very high energies and high energy thresholds of the particles involved in a cascade the processes in the field of the axes should be taken into account alone (hard cascade). The analytical solution has been derived of the cascade-theory equations for this case. When lowering the energy threshold the Bethe-Heitler processes on separate nuclei should be taken into account as well (mixed and soft cascades). These cascades are analysed using computer simulation. The results are presented concerning the recent experiments on radiation and pair creation in aligned single crystals.

1. Introduction

In /1/ the authors have pointed out the existence of particular electron-photon showers in aligned single crystals. At small angles of incidence ϑ_0 of the initial photon or electron, $\vartheta_0 \ll V_0/m$, (V_0 is the scale of the axis or plane potential), a shower takes place in the fields of separate axes (planes). Of significance is that at energies considerably exceeding the creation threshold of an electron-positron pair the shower can generate on the lengths (depending upon the substance and orientation) one or two orders of magnitude shorter than the shower in an appropriate amorphous substance, which is due to the standard interaction mechanism with individual nuclei (Bethe-Heitler mechanism). Note that this particular mechanism in question is the most effective mechanism of electromagnetic energy losses. At present, the theory is developed of pair creation /2/ and radiation /3/ which is valid at any angles of incidence and offers the possibility of tracing the dynamics of showers in aligned single crystals at any ϑ_0 . However, the maximum effects take place at small ϑ_0 and in the fields of the axes so that we will deal with this case.

The theory of cascade showers in an amorphous substance has been formulated and developed in /4-6/. In these papers the kinetic equations have been derived which describe the evolution of a cascade and the analytical solution for these equations has been found in the case when allowance is made for the radiation and pair creation processes only /6/. Note that the probabilities of the latter have been found by Bethe and Heitler (see, e.g., /7/). Subsequently, a great deal of the papers developing this theory has been published (for their review see, e.g., /6/).

Let us discuss the distinctive features of the shower in aligned single crystals. 1) As has already been mentioned, the characteristic lengths of radiation and pair creation here can be far less than in an appropriate amorphous substance (in a non-aligned crystal). 2) There is a sharp boundary (threshold) ω_t with respect to photon energies below which the probability of the pair photoproduction in the axis field falls off exponentially. We choose it in such a way that the photoproduction probability in the field is $W_e^F(\omega_t) = W_e^{BH}$ (the values of ω_t are given in /2/). At the same time, if the energy of the particle is $\varepsilon \sim \omega_t$ it emits intensively on account of the mechanism under discussion. 3) Within the $\omega > \omega_t$ region, both the pair creation probability $W_e^F(\omega)$ and the characteristic length of the energy losses $L_{ch}(\varepsilon) = \varepsilon / I(\varepsilon)$ ($I(\varepsilon)$ is the radiation intensity) are energy-dependent, while for the Bethe-Heitler process the corresponding quantities W_e^{BH} and L_{rad} are constant. 4) At $\varepsilon \lesssim \omega_t$ the total radiation probability is roughly one order of magnitude higher than the inverse characteristic length of the energy losses caused by the radiation $L_{ch}^{-1}(\varepsilon)$ (note that this probability can be found using the magnetic-bremsstrahlung limit). This means that a great amount of relatively soft quanta is emitted that exert no influence on the energy losses of a particle emitting them. Nevertheless, these photons can produce the pairs due to the Bethe-Heitler mechanism (i.e. with relatively low probability). As a result, the particular shower evolves due to a mixed mechanism at which a large number of photons can produce a noticeable number of pairs, despite a low probability of the photoproduction process. It is then natural that the number of photons in the shower will

be considerably greater than that of charged particles. In what follows we will distinguish the hard showers when the particle energy is $\varepsilon \gg \omega_t$ and soft ones when $\varepsilon \lesssim \omega_t$.

The indicated peculiarities of the evolution of the shower in an aligned crystal make it far different from the standard cascade shower in an amorphous substance /4-6/. In this case, it is impossible to use both the results derived for this case and the method of solving a kinetic equation /6/. The present paper is devoted to an analysis of the evolution of a shower in aligned single crystals. Our analysis involves an analytical solution for a hard cascade and the numerical results based on the Monte Carlo simulation of the process. Such calculations have been made for the hard and soft showers using the characteristics of the radiation and pair creation which have been derived in Refs. /1-3,9/.

2. Kinetic equations

An evolving electron-photon shower when passing through a matter is characterized by the number of photons $N_\gamma(\omega,t)$ and of charged particles $N_e(\varepsilon,t)$ with energies ω and ε, at a given depth t. The functions N_γ and N_e satisfy the following kinetic equations /6/:

$$\frac{\partial N_\gamma(\omega,t)}{\partial t} = -W(\omega)N_\gamma(\omega,t) + \int_\omega^\infty W_\gamma(\varepsilon,\omega)N_e(\varepsilon,t)\,d\varepsilon ,$$

$$\frac{\partial N_e(\varepsilon,t)}{\partial t} = -W_\gamma(\varepsilon)N_e(\varepsilon,t) + \int_\varepsilon^\infty W_\gamma(\varepsilon',\varepsilon'-\varepsilon)N_e(\varepsilon',t)\,d\varepsilon' + 2\int_\varepsilon^\infty W(\omega,\varepsilon)N_\gamma(\omega,t)\,d\omega \qquad (1)$$

where $W(\omega,\varepsilon)$ is the differential probability of the electron-positron pair creation by a photon with energy ω when the energy of one of the pair particle is ε (while that of the other is $\varepsilon' = \omega - \varepsilon$), $W(\omega)$ is the total pair creation probability, $W_\gamma(\varepsilon,\omega)$ is the differential emission probability of a photon with energy ω by a charged particle with energy ε, $W_\gamma(\varepsilon)=\int_0^\varepsilon W_\gamma(\varepsilon,\omega)\,d\omega$ is the total radiation probability*). It is convenient to introduce new functions $\nu(\varepsilon,t)$ and $N_0(\varepsilon';\varepsilon,t)$ defined as follows:

$$\frac{\partial N_0(\varepsilon';\varepsilon,t)}{\partial t}=-W_\gamma(\varepsilon)N_0(\varepsilon';\varepsilon,t)+\int_\varepsilon^\infty W_\gamma(\varepsilon'',\varepsilon''-\varepsilon)N_0(\varepsilon';\varepsilon'',t)\,d\varepsilon'', \tag{2}$$

$$N_0(\varepsilon';\varepsilon,0)=\delta(\varepsilon-\varepsilon'),$$
$$N_e(\varepsilon,t)=\int_0^t d\tau\int_\varepsilon^\infty \nu(\varepsilon',t-\tau)N_0(\varepsilon';\varepsilon,\tau)\,d\varepsilon' \tag{3}$$

It is seen from the definitions (2) and (3), that the distribution function $N_0(\varepsilon';\varepsilon,t)$ is only connected with the radiation kinetics, while $\nu(\varepsilon,t)$ characterizes the source of electron-positron pair. Note that it follows from (2) that

$$\int_0^{\varepsilon'} N_0(\varepsilon';\varepsilon,t)\,d\varepsilon=1 .$$

With (2) and (3) substituted into (1) we find

$$\frac{\partial N_\gamma(\omega,t)}{\partial t}=-W(\omega)N_\gamma(\omega,t)+\int_\omega^\infty d\varepsilon\int_0^t d\tau\,\nu(\varepsilon,t-\tau)W_\gamma(\varepsilon,\omega,\tau), \tag{4}$$
$$\nu(\varepsilon,t)=2\int_\varepsilon^\infty W(\omega,\varepsilon)N_\gamma(\omega,t)\,d\omega ,$$

where

$$W_\gamma(\varepsilon,\omega,\tau)=\int_\omega^\varepsilon W_\gamma(\varepsilon',\omega)N_0(\varepsilon;\varepsilon',\tau)\,d\varepsilon' \tag{5}$$

Substituting the second of equations (4) into the first, we have the final equation for $N_\gamma(\omega,t)$:

*) In eqs. (1) the electrons and positrons are assumed to radiate in the same manner. This holds in the case of uniform distribution with respect to the transverse coordinates (see Ref. /3/).

$$\frac{\partial N_\gamma(\omega,t)}{\partial t}=-W(\omega)N_\gamma(\omega,t)+2\int_\omega^\infty d\varepsilon\int_\varepsilon^\infty d\omega'\int_0^t d\tau\, W(\omega',\varepsilon)\cdot$$
$$\cdot W_\gamma(\varepsilon,\omega,\tau)N_\gamma(\omega',t-\tau) \tag{6}$$

Equation (6) is exact. We will solve it making certain simplifications. An important step consists in the following replacement:

$$W_\gamma(\varepsilon,\omega,\tau)=W_\gamma(\varepsilon(\tau),\omega),$$
$$\frac{d\varepsilon(\tau)}{d\tau}=-I(\varepsilon(\tau)), \tag{7}$$

where $I(\varepsilon)$ is the radiation intensity of a particle with energy ε. In this case we neglect the energy dispersion of the electrons upon radiation. Strictly speaking, this is prohibitive in the calculation of the energy distribution of electrons itself in the course of the radiation. When calculating the energy losses the replacement (7) however is quite justified*) /9/. Equations (6) and (7) are far simpler than the initial (1) and this makes possible further progress in their solution for the case when the radiation and pair creation probabilities are considerably different from the Bethe-Heitler ones.

The next step is to simplify the expressions for the differential radiation and pair creation probabilities. We define them using the equalities

$$W(\omega,\varepsilon)=W(\omega)\,\frac{\vartheta(\omega-\varepsilon)}{\omega},$$
$$W_\gamma(\varepsilon,\omega)=L_{ch}^{-1}(\varepsilon)\,\frac{\vartheta(\varepsilon-\omega)}{\omega} \tag{8}$$

here $L_{ch}^{-1}(\varepsilon)=-\frac{1}{\varepsilon}\frac{\partial\varepsilon}{\partial t}$. The characteristic radiation length $L_{ch}(\varepsilon)$

*) For the standard Bethe-Heitler shower this replacement results in an error in a few per cent (cf., for example, /7/).

and the pair creation probability $W(\omega)$ are presented in Refs. /1-3,9/. Below we will restrict ourselves to the situation when the constant-field limit is applicable for these quantities. This limit is true (see Refs. /2,3/) under the condition that the angle of particle motion is $\vartheta \lesssim \frac{V_0}{m}$, with respect to the axis. At $\varepsilon, \omega \gtrsim \omega_t$ it suffices if the angle of incidence ϑ_0 of the initial particle satisfies this condition since the characteristic angles of radiation and pair creation are $\vartheta_r \sim \frac{m}{\varepsilon} \ll \frac{V_0}{m}$ for this case. The analysis made for the Bethe-Heitler cascade shows that the replacement (8) also has little influence on the characteristics of the shower (the error constitutes a few per cent). As a result, the substitutions (7) and (8) give rise for the Bethe-Heitler cascade to a 10% discrepance with Landau-Rumer's solution /6/. In case of a hard shower in single crystals when $\omega, \varepsilon \gg \omega_t$, the probabilities $W_\gamma(\varepsilon,\omega)$ and $W(\omega,\varepsilon)$ are similar, in form, to the Bethe-Heitler ones /2,3/ and, hence, the substitution (8) is admissible, with the indicated accuracy.

Let us introduce the following variables and functions:

$$\eta = \ln\frac{\omega_0}{\omega}, \quad \zeta = \ln\frac{\omega_0}{\varepsilon}, \quad a(\zeta) = L_{ch}^{-1}(\omega_0 e^{-\zeta}),$$
$$b(\eta) = W(\omega_0 e^{-\eta}), \; N(\omega,t) = \frac{1}{\omega_0} N(\eta,t), \; n(\eta,t) = e^{-\eta} N(\eta,t), \tag{9}$$

where ω_0 is the energy of the initial particle, for example, of a photon. With (7)-(9) substituted into (6), we get

$$n_t + b(\eta) n = 2 \int_0^t d\tau \int_0^\eta d\zeta \int_0^\zeta d\eta' e^{\eta' - \zeta} a(\zeta(\tau)) b(\eta') \cdot$$
$$\cdot\, n(\eta', t-\tau)\, \vartheta(\eta - \zeta(\tau)), \tag{10}$$

where $n_t \equiv \frac{\partial n}{\partial t}$. Of interest is the region $t \gg L_{ch}(\varepsilon_0)$ wherein the cascade has time to evolve to a considerable extent. Here the characteristic values of the quantities are $\eta, \zeta \gg 1$. It is the region we will consider below. In the energy range where

the hard cascade occurs the functions $a(\zeta)$ and $b(\eta)$ are very smooth /2,3/. Therefore, the assumption can be made that the derivatives $a'(\zeta)$ and $b'(\eta)$ may be ignored.

Let us now transform equation (10) acting on it by the operator $\frac{\partial}{\partial t} + a(\eta)\frac{\partial}{\partial \eta}$ and bearing in mind that the main contribution to the right-hand side comes from $\eta - \zeta, \eta - \eta' \sim 1$. With the above assumptions taken into account, we derive the final form of the kinetic equation:

$$n_{tt} + a(\eta)\left(n_{\eta t} + b(\eta) n_\eta\right) + b(\eta) n_t =$$
$$= 2a(\eta) b(\eta) \int_0^\eta d\zeta \int_0^\zeta d\eta' e^{\eta' - \zeta} n(\eta', t) =$$
$$= 2a(\eta) b(\eta) \int_0^\eta dy (1 - e^{-y}) n(\eta - y, t). \tag{11}$$

3. Solution of the kinetic equation

As is well known, the number of particles in a cascade grows exponentially as it evolves in a substance. In view of this, the solution of eq. (11) will be seeked in the form $n(\eta,t) = A(\eta,t)\exp[f(t)]$. Introducing the notations $\frac{\partial f}{\partial t} \equiv f_t = \mu$ and $\frac{\partial f}{\partial \eta} \equiv f_\eta = \lambda$, neglecting the derivatives of A and the second ones of f (these terms are $\sim 1/\eta$), expanding the exponent in $n(\eta - y, t)$ with respect to y and, finally, taking the corresponding integral in (11), we obtain for μ and λ the following equation

$$\lambda(\lambda+1)(\mu+b)(\mu+a\lambda) = 2ab \tag{12}$$

The solution of this partial differential equation of the first-order is of the form

$$f(\eta,t) = F(\mu,\eta,t) = \mu t + \int_0^\eta \lambda(\mu, a(y), b(y))\, dy$$

where $\mu = \mu(\eta, t)$ is found from the condition $\frac{\partial F}{\partial \mu} = 0$. The corresponding expression for $n(\eta, t)$ is convenient to represent as a contour integral which is to evaluate using the saddle-point method:

$$n(\eta, t) = \frac{1}{2\pi i} \int_{c-i\infty}^{c+i\infty} d\mu\, C(\mu, \lambda, a(\eta), b(\eta)) \exp\Big[\mu t + \int_0^\eta \lambda(\mu, a(y), b(y))\, dy\Big] \qquad (13)$$

According to what has been said above, the derivatives of $a(\eta)$ and $b(\eta)$ will be neglected when substituting (13) into eq. (11). To solve eq. (11) it is necessary now to find an explicit form of the function C in (13) in accord with the initial conditions. To do this, it suffices to solve the problem with constant a and b. In this case, eq. (11) is solved using the Laplace transform with respect to the variable η. In the case when the initial particle is a photon, the exponentially increasing at large t part of the solution is as follows:

$$n^{(\gamma)}(\eta, t) = \frac{1}{2\pi i} \int_{c-i\infty}^{c+i\infty} \frac{\mu + \lambda a}{2\mu + \lambda a + b} e^{\mu t + \lambda \eta} d\lambda \qquad (14)$$

Note that $\mu = \mu(\lambda)$ is one of the roots of eq. (12), namely:

$$\mu(\lambda) = -\frac{b + \lambda a}{2} + \sqrt{\frac{(\lambda a - b)^2}{4} + \frac{2ab}{\lambda(\lambda+1)}} \qquad (15)$$

From the comparison of (13) and (14) we find that

$$C^{(\gamma)}(\mu, \lambda, a(\eta), b(\eta)) = -\frac{\lambda_\mu (\mu + \lambda a)}{2\mu + \lambda a + b}, \quad \lambda_\mu \equiv \frac{\partial \lambda}{\partial \mu} \qquad (16)$$

At large $t \gg a^{-1} = L_{ch}$ the integral (13) is taken using the saddle-point method. As a result, we have for the number of photons at a large depth t:

$$N_\gamma^{(\gamma)}(\eta, t) = -\frac{\lambda_\mu (\mu + \lambda a)}{\sqrt{2\pi d}\,(2\mu + \lambda a + b)} \exp\Big[\mu t + \eta + \int_0^\eta \lambda(\mu, a(y), b(y))\, dy\Big], \qquad (17)$$

where

$$t + \int_0^\eta \lambda_\mu (\mu, a(y), b(y))\, dy = 0$$
$$d = \int_0^\eta \lambda_{\mu\mu} (\mu, a(y), b(y))\, dy \qquad (18)$$

The first of the equalities (18) defines μ as a function of t and η ($\mu = \mu(\eta, t)$). Using (4) and (3) and taking (7) into account ($N_0(\varepsilon'; \varepsilon, \tau) = \delta(\varepsilon'(\tau) - \varepsilon)$) we have, with the same accuracy, the expression for the number of charged particles:

$$N_e(\eta, t) = \frac{2b}{(\lambda+1)(\mu + \lambda a)} N_\gamma(\eta, t) = (\mu + b)\frac{\lambda}{a} N_\gamma(\eta, t) \qquad (19)$$

If the initial particle is an electron (positron) with energy ε_0, the number of the photons with an energy ω ($\eta = \ln \frac{\varepsilon_0}{\omega}$) is found from the expression

$$N_\gamma^{(e)}(\eta, t) = -\frac{\lambda_\mu a}{\sqrt{2\pi d}\, \lambda (2\mu + \lambda a + b)} \cdot \exp\Big[\mu t + \eta + \int_0^\eta \lambda(\mu, a(y), b(y))\, dy\Big] \qquad (20)$$

Of course the relation (19) holds in this case.

Of great interest is the total number of the particles $\Pi(\eta_f, t)$ with energy $\omega, \varepsilon \geq \varepsilon_f$, $\eta_f = \ln \frac{\varepsilon_0}{\varepsilon_f}$. To find $\Pi(\eta_f, t)$ the function $N(\eta', t)$ should be integrated over η' with the weight $e^{-\eta'}$ ($-d\omega = \varepsilon_0 d\eta' e^{-\eta'}$). With the accepted accuracy, the calculation can be made, by expanding the index in (17) near the point $\eta' = \eta$ and by proceeding to the integration variable $\eta' - \eta$. Taking the first of the equalities (18) into account, we obtain

$$\Pi(\eta_f,t) = \int_0^{\eta_f} N(\eta',t)e^{-\eta'}d\eta' = \frac{e^{-\eta_f}}{\lambda}N(\eta_f,t) \quad (21)$$

Making allowance for (18) it is easy to see that a maximum number of the particles, at fixed η, is achieved at $t = t_{op}$ defined from the condition $\mu(\eta,t) = 0$. From Eq. (12) (the branch (15)) we get $\lambda = 1$ at $\mu = 0$. for any a and b. Calculating λ_μ and $\lambda_{\mu\mu}$ at the point $\lambda = 1$ and $\mu = 0$ we find

$$\lambda_\mu(\mu=0) = -\frac{2(a+b)}{5ab}, \quad \lambda_{\mu\mu}(\mu=0) = \frac{4}{125}\left(\frac{7}{a^2} - \frac{1}{ab} + \frac{17}{b^2}\right) \quad (22)$$

For t_{op} we then obtain from (18)

$$t_{op} = \frac{2}{5}\int_0^{\eta} dy\left(\frac{1}{a(y)} + \frac{1}{b(y)}\right) \quad (23)$$

At t close to t_{op}, the main contribution to the integral over μ comes from the vicinity of the point $\mu = 0$. Expanding the exponent argument in (13) with due regard for the relation (22) and taking the integrals, we derive the explicit expressions for the distribution functions $N_\gamma(\eta,t)$ and $N_e(\eta,t)$ which are of the form gaussian distribution in time (depth):

$$N_\gamma(\eta,t) = \frac{2}{5}\frac{e^{2\eta}}{\sqrt{2\pi d}\, b(\eta)}\exp\left[-\frac{(t-t_{op})^2}{2d(\eta)}\right], \quad N_e(\eta,t) = \frac{b(\eta)}{a(\eta)}N_\gamma(\eta,t),$$
$$d(\eta) = \frac{4}{125}\int_0^{\eta} dy\left(\frac{7}{a^2(y)} - \frac{1}{a(y)b(y)} + \frac{17}{b^2(y)}\right). \quad (24)$$

For electron-photon showers in an amorphous substance ($\frac{b}{a} = \frac{7}{9}$, $a^{-1} = L_{rad}$) we have

$$N_\gamma(\eta,t_{op}) = \frac{0.197}{\sqrt{\eta}}e^{2\eta}, \quad N_e(\eta,t_{op}) = \frac{0.153}{\sqrt{\eta}}e^{2\eta},$$
$$t_{op} = \frac{32}{35}\eta L_{rad} \quad (25)$$

This is in good agreement (the difference is $\simeq 10\%$) with the standard shower theory. Note that our computer simulation of the hard cascade is well consistent with the results of the preceding analytical calculation.

4. Results

Besides the hard cascade (when the particle and photon energy is $\varepsilon, \omega \gg \omega_t$) whose evolution is analytically analysed in the foregoing section, a situation is possible when the lower energy boundary is $\varepsilon_f(\omega_f) \ll \omega_t$. In this case, at a photon energy $\omega \lesssim \omega_t$ the Bethe-Heitler mechanism of pair creation basically works, while the particle radiation in the field of an aligned single crystal still remains rather intense ($b \simeq W_e^{BH}$, $a \gg L_{rad}^{-1}$).

It is obvious that the major part of photons is emitted on the characteristic length $l \sim \int_0^{\eta}\frac{dy}{a(y)} = \int_0^{\eta} L_{ch}(\varepsilon_0 e^{-y})dy \ll t_{op}$ and there is a wide enough interval wherein the number of photons remains practically constant (smoothly reducing on account of the absorption) up to the length $t \sim (W_e^{BH})^{-1}$ when a noticeable photon absorption starts due to a transformation into the e^+e^- pairs. In the situation under analysis, two essentially different cases can take place. In the first case, the initial energy is $\omega_0(\varepsilon_0) \gg \omega_t$ and the mixed cascade develops, while in the second one $\omega_0(\varepsilon_0) \sim \omega_t$ and the soft cascade develops.

We would like to start with the results of the computer simulation concerning the mixed cascade. The simulation has been performed for a silicon crystal oriented along the $\langle 110 \rangle$ axis and at $T = 293$ K. Fig. 1 shows the number of the charged particles and photons against the depth ℓ at which the shower evolves in the crystal, for various energies of the initial photon. The lower boundary of the photon energy in the cascade is taken to be $\omega_f = 100$ MeV and it corresponds roughly to the effective threshold of electron-positron pair creation in a substance. It is seen from Fig. 1 that the number of the photons reaches the plateau, in agreement with the said above. The lower boundary for the charged-particle energy is taken equal to $\varepsilon_f = 10$ GeV. On the one hand, this choice ensures the applicability of the employed magnetic bremsstrahlung approximation, and, on the other hand, at $\varepsilon < 10$ GeV the photons are basically emitted whose energy is $\omega < \omega_f = 100$ MeV. The presented results allow one to optimize the crystal thickness in the crystal-based, ultrahigh-energy electron and photon detector suggested by the authors [10].

Fig. 2 illustrates the number N_γ of the photons with $\omega > 100$ MeV and the total number of the charged particles N_e vs. the energy ω_0 of the initial photon incident on a Si crystal of thickness $L = 1$ cm at a small angle $\vartheta_0 \ll \frac{V_0}{m}$ to the $\langle 110 \rangle$ axis. It is interesting that the ratio of the number of photons N_γ to that of charged particles N_e does not practically depend on the initial energy and is $N_\gamma / N_e \sim 11$. The curves in Fig. 2 permit one to find with good accuracy /10/ the energy of superhard photons, upon detection. As the photon energy grows, it turns out to be sufficient for this purpose, to detect the charged particles only, without additional devices for the photon-into e^-e^+ pairs conversion.

Fig. 3 demonstrates the energy distributions of the pho-

tons for various energies of the initial photon.

In the case when the initial particle (photon) energy is of the order of the threshold energy ω_t, the soft cascade develops wherein, as already mentioned, emission of a great number of photons lead to the creation of a noticeable number of the e^+e^- pairs despite the quantity W_e^{BH} is small. In this case, for $\ell \lesssim L_{ch} \ll L_{rad}$ the method of successive approximations is suited for an analytical calculation inasmuch as the relative amount of the secondary particles is small. For example, within the framework of the accepted approach we find the number of the photons at a depth ℓ, for the initial electron

$$N_\gamma^{(e)}(\ell) = \int_0^\ell W_\gamma(t)dt = \int_{\varepsilon(\ell)}^{\varepsilon_0} W_\gamma(\varepsilon) L_{ch}(\varepsilon) \frac{d\varepsilon}{\varepsilon} = \int_0^\eta \frac{W_\gamma(\varepsilon_0 e^{-y})}{d(y)} dy \simeq \overline{W_\gamma}\,\ell \ , \ \eta = \ln\frac{\varepsilon_0}{\varepsilon(\ell)} \quad (26)$$

The latter equality in formula (26) is satisfied with good accuracy due to a weak dependence of the total radiation probability W_γ on ε in the energy range under consideration. In this range a magnetic bremsstrahlung description is valid, and the quantum effects for the total probability are still relatively small. Correspondingly, for the number of secondary charged particles we obtain

$$N_e^{(e)}(\ell) = 2\int_0^\ell W_e^{BH} N_\gamma(t)dt = 2W_e^{BH}\int_0^\ell W_\gamma(t)(\ell - t)dt \simeq W_e^{BH}\overline{W_\gamma}\,\ell^2 \simeq W_e^{BH} N_\gamma^{(e)}(\ell)\,\ell \quad (27)$$

One can in principle to calculate the terms of the next approximations as well. At $\ell \ll L_{ch}$ these terms are however small, whereas at $\ell \gtrsim L_{ch}$ the secondary particles are produced mainly with an energy lower than the threshold ε_f.

Recently the experiments have been made on electron radiation and pair creation by photons in a single crystal at a high enough particle energy /11,12/ when the particular shower may manifest itself. In the experiment /11,12/ Ge single crystals of thickness L = 0.4 and 1.4 mm, cooled down to 100 K were used. The initial electrons with ε_o = 150 GeV and the photons with ω_o < 155 GeV have been incident on the single crystal in the direction around the ⟨110⟩ axis. Bearing in mind that for these conditions ω_t = 50 GeV [13,2] this experimental situation can be referred to the case of soft cascade.

We would like to discuss first the case when the initial particle is an electron. The first estimate of the mean energy losses caused by the radiation has been obtained*) in Ref. /13/. The radiation characteristics with regard for the energy losses has been analysed in detail in Ref. /9/. However, no allowance has been made in that paper for the creation of secondary particles whose number can be estimated according to formulae (26)-(27). For L = 1.4 mm, one has**) $\overline{W_\gamma}$ = 120 cm^{-1}, $\overline{W_e^{BH}}$ = 0.28 cm^{-1}. From (26) and (27) we then have

$$\mathcal{N}_\gamma^{(e)}(L) \simeq 16.8 \quad , \quad \mathcal{N}_e^{(e)}(L) \simeq 0.67 \qquad (28)$$

Taking into account consideration that for L = 0.4 mm, $\overline{W_\gamma}$ = 111 cm^{-1}, we find the number of photons and secondary electrons for this thickness:

$$\mathcal{N}_\gamma^{(e)}(L) \simeq 4.4 \quad , \quad \mathcal{N}_e^{(e)}(L) \simeq \frac{1}{20} \qquad (29)$$

We have made a numerical calculation of the cascade for the experimental conditions indicated in Refs. /11,12/. For the number of the photons whose energy is higher than ω_f = 100 MeV we have obtained $\mathcal{N}_\gamma(1.4) \simeq 13.9$ and $\mathcal{N}_\gamma(0.4) \simeq 3.9$, while for the total number of photons the results are: $\mathcal{N}_\gamma(1.4) \simeq 17.3$ and $\mathcal{N}_\gamma(0.4) \simeq 4.4$; the results obtained are well consistent with the estimates (28) and (29). The agreement is also good for the number of secondary particles.

Fig. 4 illustrates the averaged over crystal thickness spectral radiation intensity obtained from the computer simulation; it being in good agreement with the results of Ref. /9/. Thus, the use of $\mathcal{N}_o(\varepsilon;\varepsilon',\tau)$ as $\delta(\varepsilon'(\tau)-\varepsilon)$ is now justified. As has already been mentioned in Ref. /9/, due to the fact that the particle emits several photons and the detector has registered their total energy in the experiment of Ref. /11/, the distribution has really been measured with respect to the energy losses of the incident electrons rather than the spectral distribution of radiation. Fig. 5 presents the computational results on energy distribution of charged particles for ε > 5 GeV. Note that despite a considerable number of the secondary particles (see eq. (28)), most of them have the energy ε < 5 GeV and, hence, they have no influence in practice on the spectrum for ε > 5 GeV. In view of this, the results in Fig. 5 can be directly compared with the distribution in Fig. 2 in Ref. /11/ (with a substitution $x \to 1-x$). It is seen that the results of our calculation are well consistent with the experiment /11/. With the found distributions we obtain for the

---

*) The published later experimental data (Ref. /11/) have shown that this estimate agrees quite satisfactorily with the experiment.

**) The value of $\overline{W_e^{BH}}$ is taken with regard for thermal vibrations, just as in Ref. /13/.

average energy of electrons with $\varepsilon > 5$ GeV, at the exit from the crystal $\bar{\varepsilon} = 0.26\varepsilon_0$ at $L = 1.4$ mm, and, correspondingly, $\bar{\varepsilon} = 0.66\,\varepsilon_0$ at $L = 0.4$ mm. These velues are nearly the same as those in Ref. /9/ and the experimental results (Refs. [11,12]).

We have analysed also the case when the photon with energy ω_0 is incident on the crystal and the electron-positron pair creation has been studied under the conditions of the experiment*) /12/. Curves 1 and 2 show the spectral distribution of the electrons (positrons) produced by a photon with $\omega_0 = 150$ GeV and $\omega_0 = 100$ GeV, with their further radiation neglected. The calculation of this distribution within the framework of the cascade theory for the same initial photons (curves 3,4 in Fig. 6) demonstrate a dramatic difference of the spectra of the produced particles in a crystal of thickness $L = 1.4$ mm in comparison with the spectrum which would be observed in a very thin crystal (curves 1,2). If one considers the radiation of the photons with $\omega > 100$ MeV, at $\omega_0 = 150$ GeV we then have $N_\gamma \simeq 4.8$, while for $\omega_0 = 100$ GeV we have $N_\gamma \simeq 3.4$. The total number of the photons is 6 and 4.4 respectively. Thus, from the analysis it follows that already under the experimental conditions Refs. /11,12/) the cascade processes should be taken into account.

We would like to express our gratitude to V.A.Taurski for the help with numerical calculations.

---

*) Emphasize that according to the recent data /14/ the total e^+e^- - pair creation probability is in a good agreement with theory; the sum $W = W_e^F(\omega_0) + W_e^{BH}$ was used as theoretical prediction. For the experimental conditions [12] the value of $W_e^F(\omega_0)$ is given in Fig. 1 in Ref. /13/.

References

1. V.N.Baier, V.M.Katkov and V.M.Strakhovenko. Dokl. Akad. Nauk SSSR 282 (1985) 851.
2. V.N.Baier, V.M.Katkov and V.M.Strakhovenko. Zh. Eksp. Theor. Fiz. 90 (1986) 801; Nucl. Instr. and Meth. B16 (1986) 5.
3. V.N.Baier, V.M.Katkov, V.M.Strakhovenko. Preprint IJaF 86-43, 1986; Phys. Lett 117A(1986)251.
4. H.Bhabha and W.Heitler. Proc. Roy. Soc. 159 (1937) 432.
5. I.Carlson and R.Oppenheimer. Phys. Rev. 51(1937)220.
6. L.Landau and Yu.Rumer. Proc. Roy. Soc. 166(1938)213.
7. V.P.Berestetsky, E.M.Lifshits and L.P.Pitaevsky. Relativistic Quantum Theory part I (Pergamon, New York, 1971).
8. B.Rossi, High Energy Particles. New York, 1952.
9. V.N.Baier, V.M.Katkov, V.M.Strakhovenko. Phys. Lett. 114A (1986)511.
10. V.N.Baier, V.M.Katkov, V.M.Strakhovenko. Preprint IJaF 86-35, 1986; Nucl. Instr. and Meth. A250(1986)514.
11. A.Belkacem et al. Phys. Rev. Lett. 54(1985)2667.
12. A.Belkacem et al. Nucl. Instr. and Meth. B13 (1986) 9.
13. V.N.Baier, V.M.Katkov, V.M.Strakhovenko. Phys. Lett. 109A (1985)179.
14. A.Belkacem et al. Workshop "Relativistic Channeling", Italy, 1986.

Figure Captions

Fig. 1. The number of charged particles with $\varepsilon > 10$ GeV in the Si crystal (the $\langle 110 \rangle$ axis, T = 293 K) in the case when the photon with $\omega_0 = 0.4$ TeV is incident on the crystal (curve 1), $\omega_0 = 1$ TeV (curve 2) and $\omega_0 =$ = 4 TeV (curve 3). For the same conditions, curves 4,5 and 6 show the number of the photons with $\omega > 100$ MeV.

Fig. 2. The total number N_e of charged particles and photons with $\omega > 100$ MeV (N_γ) at a depth of 1 cm in the Si aligned single crystal (the $\langle 110 \rangle$ axis, T = 293 K) depending on the initial-photon energy ω_0.

Fig. 3. The energy distribution of photons at a 1 cm depth in the Si aligned single crystal (the $\langle 110 \rangle$ axis, T = = 293 K) for the initial-photon energy $\omega_0 = 0.4$ TeV (curve 1), $\omega_0 = 1$ TeV (curve 2) and $\omega_0 = 4$ TeV (curve 3).

Fig. 4. The average intensity: $\frac{dI}{d\omega} = \frac{1}{L}\frac{dN_\gamma(\omega)}{d\omega}\cdot\omega$ where L is the crystal thickness, $N_\gamma(\omega)$ is the number of the photons with energy ω leaving the Ge crystal (the $\langle 110 \rangle$ axis, T = 100 K). Curve 1 is for the initial electron with $\varepsilon_0 = 150$ GeV (L = 0.4 mm) and curve 2 is for L = 1.4 mm. Curve 3 is for the initial photon with $\omega_0 = 150$ GeV and L = 1.4 mm and curve 4 is for photon with $\omega_0 = 100$ GeV and L = 1.4 mm.

Fig. 5. The energy distribution of the charged particles leaving the Ge crystal for the initial electron with $\varepsilon_0 =$ = 150 GeV (the $\langle 110 \rangle$ axis, T = 100 K); the thickness is L = 0.4 mm (curve 1) and L = 1.4 mm (curve 2).

Fig. 6. The energy distribution of electrons at the exit of the Ge single crystal (the $\langle 110 \rangle$ axis, T = 100 K, L = 1.4 mm) if the initial photon has the energy $\omega_0 = 150$ GeV (curve 3) and $\omega_0 = 100$ GeV (curve 4). For comparison, the same distribution is given in a direct e^+e^- pair creation process for $\omega_0 = 150$ GeV (curve 1) and $\omega_0 = 100$ GeV (curve 2).

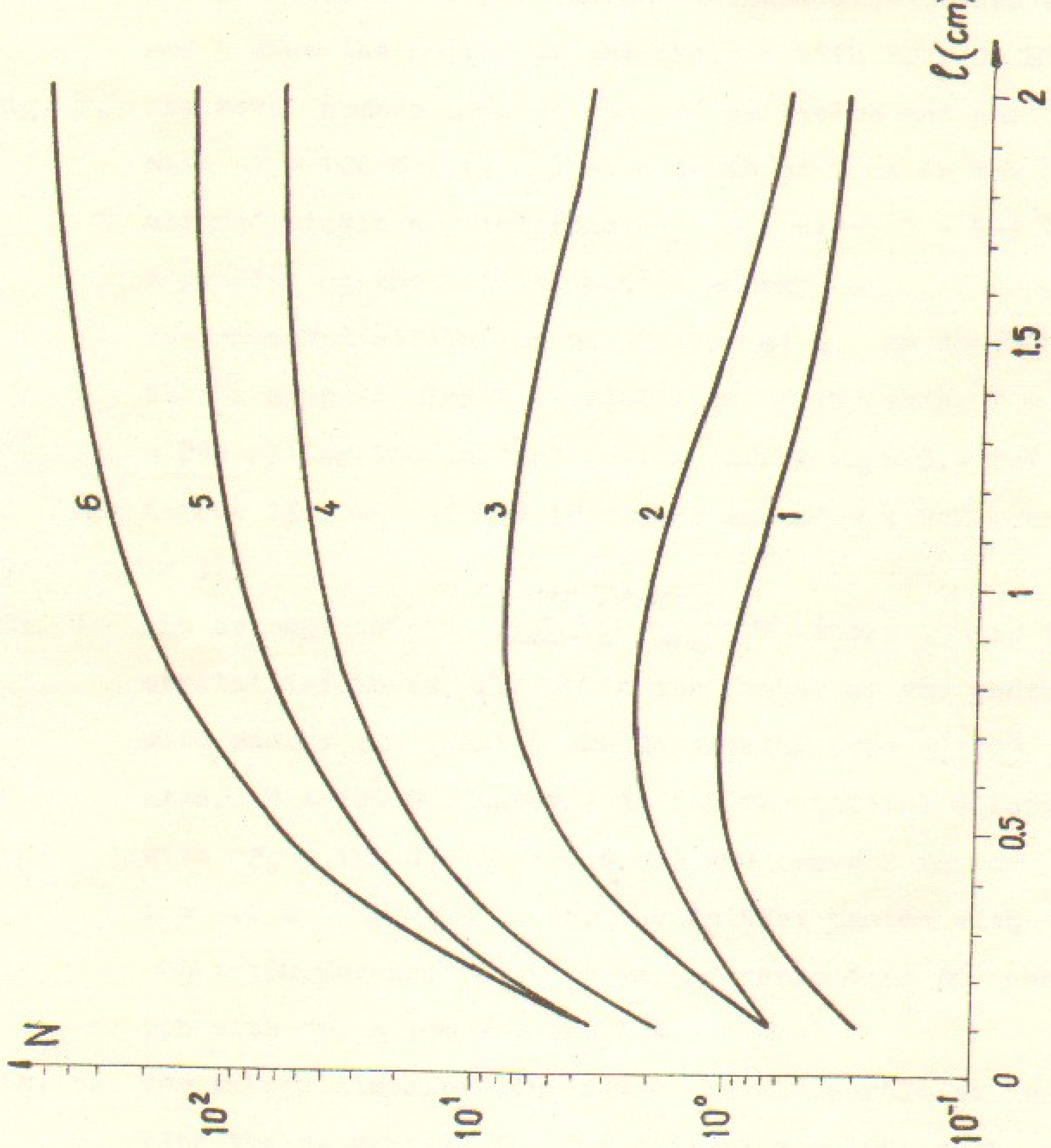
N
10^2
10^1
10^0
10^{-1}
0
0.5
1
1.5
2
ℓ(cm)
1
2
3
4
5
6

Fig.1

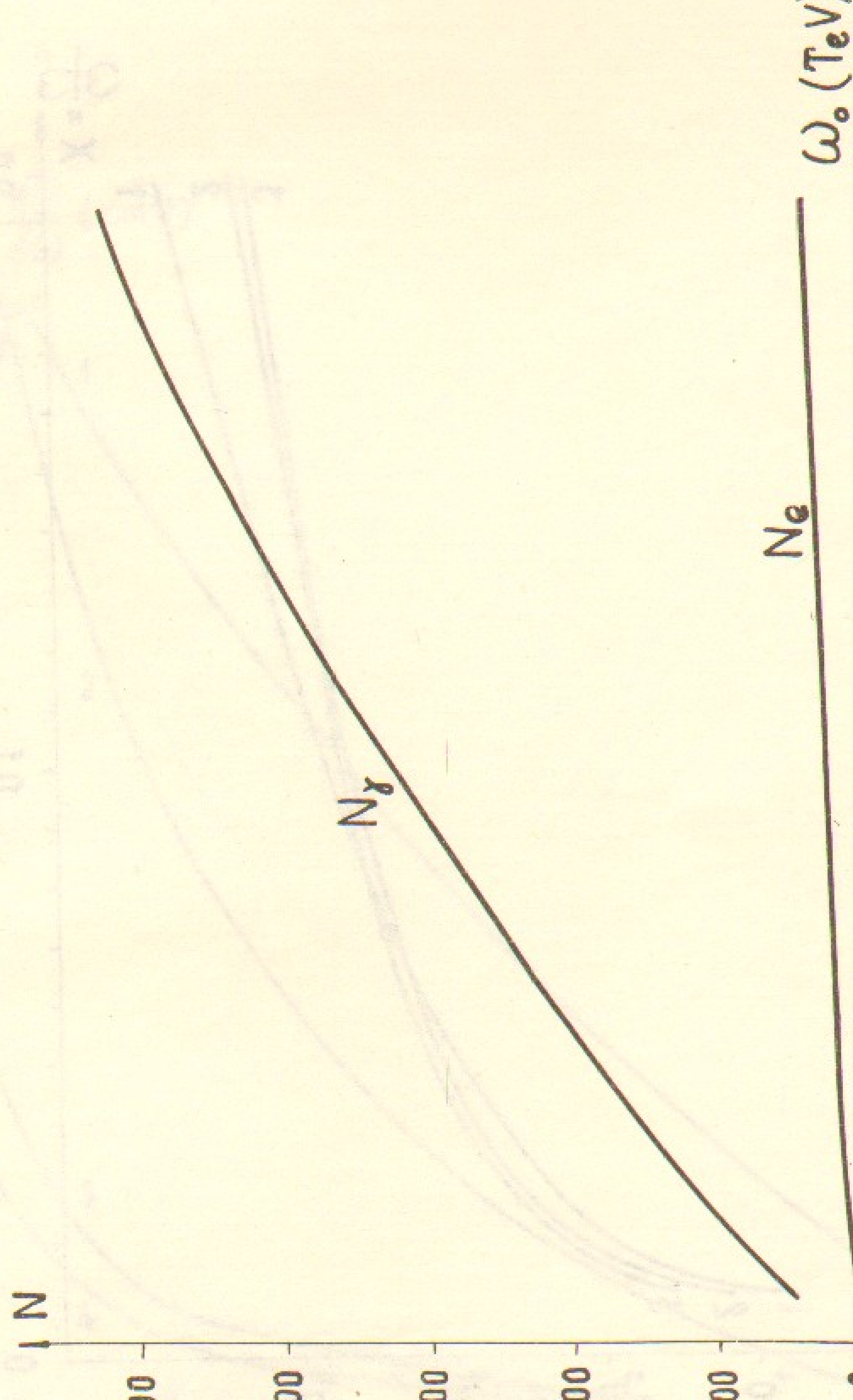
N
500
400
300
200
100
0
0
1
2
3
4
5
6
7
8
9
10
ω_o (TeV)
N_γ
N_e

Fig.2

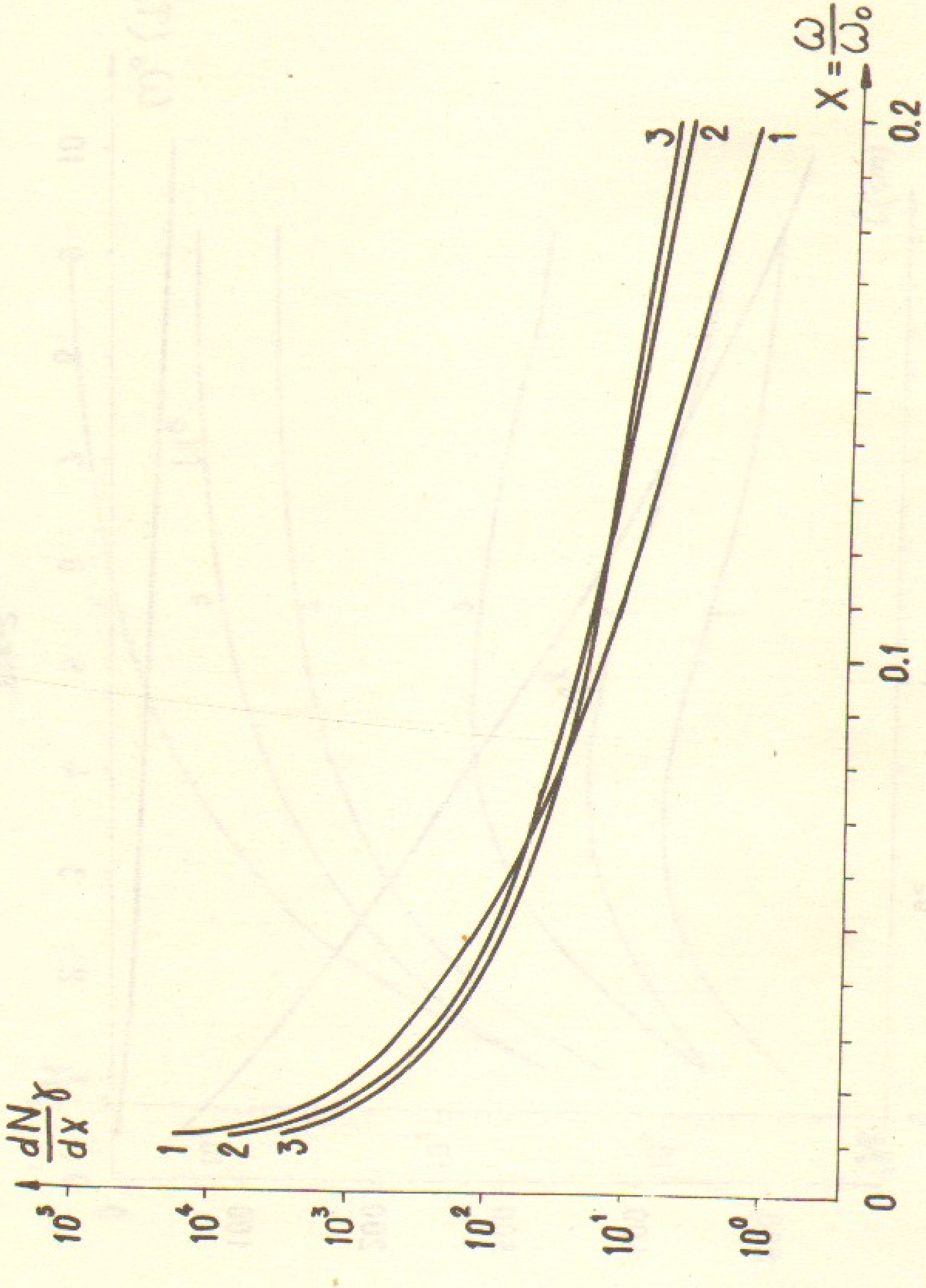

$\frac{dN}{dx}\gamma$
$X = \frac{\omega}{\omega_0}$
10^5
10^4
10^3
10^2
10^1
10^0
0
0.1
0.2
1
2
3

Fig.3

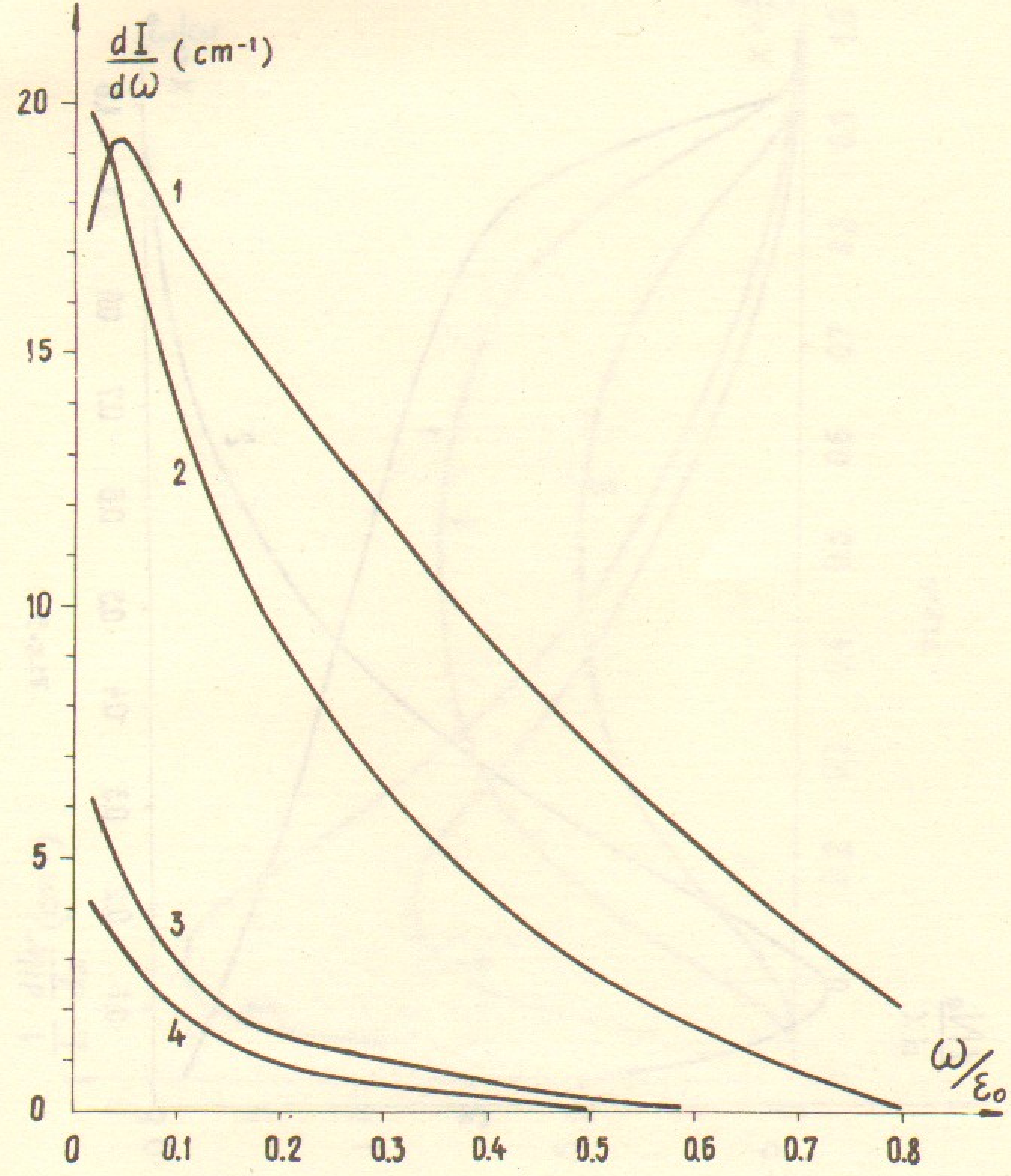

$\frac{dI}{d\omega}$ (cm^{-1})
20
15
10
5
0
0.1
0.2
0.3
0.4
0.5
0.6
0.7
0.8
ω/ε_0
1
2
3
4

Fig.4

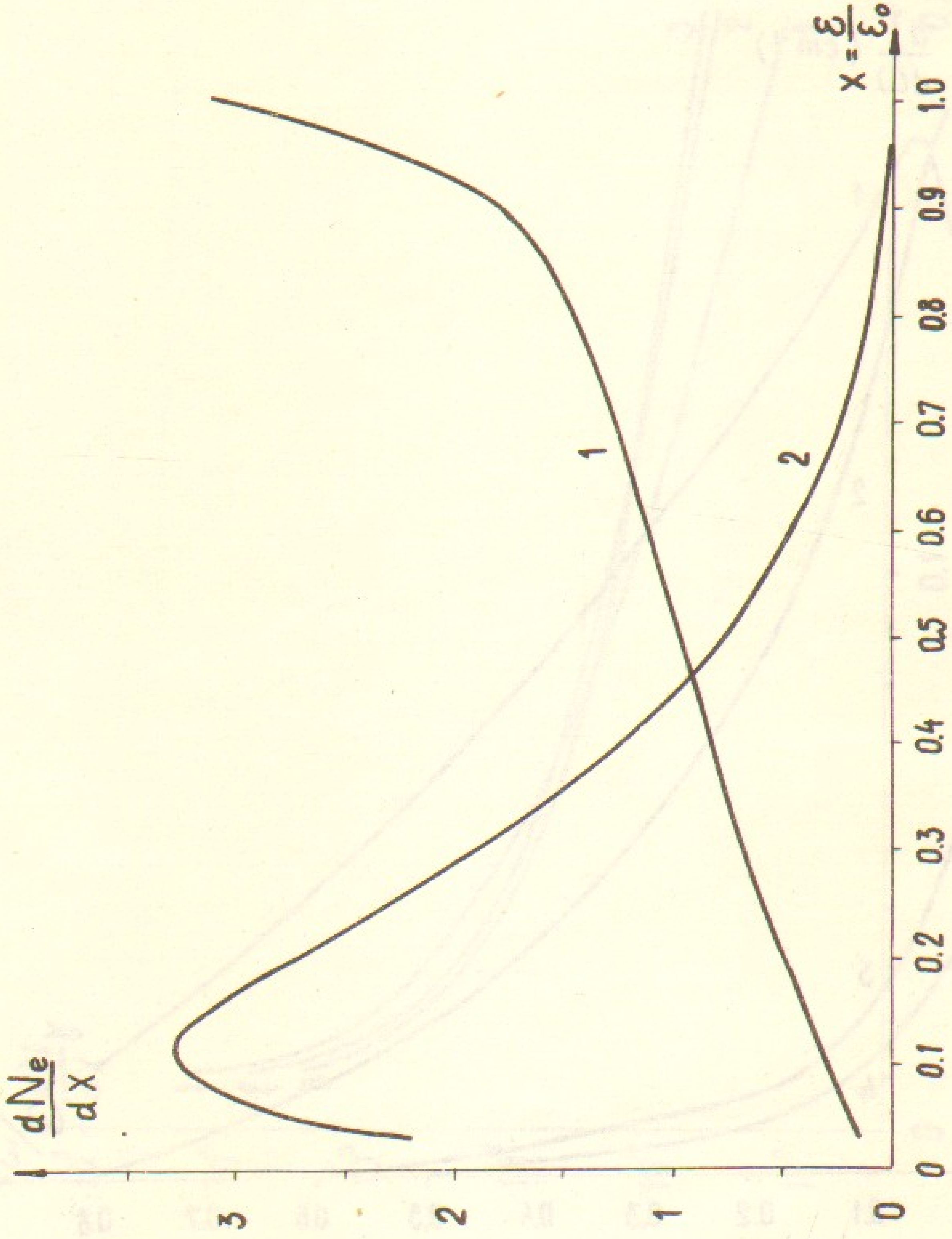
dNe / dX
X = ε / ε₀
0
1
2
3
0.1
0.2
0.3
0.4
0.5
0.6
0.7
0.8
0.9
1.0
1
2

Fig.5

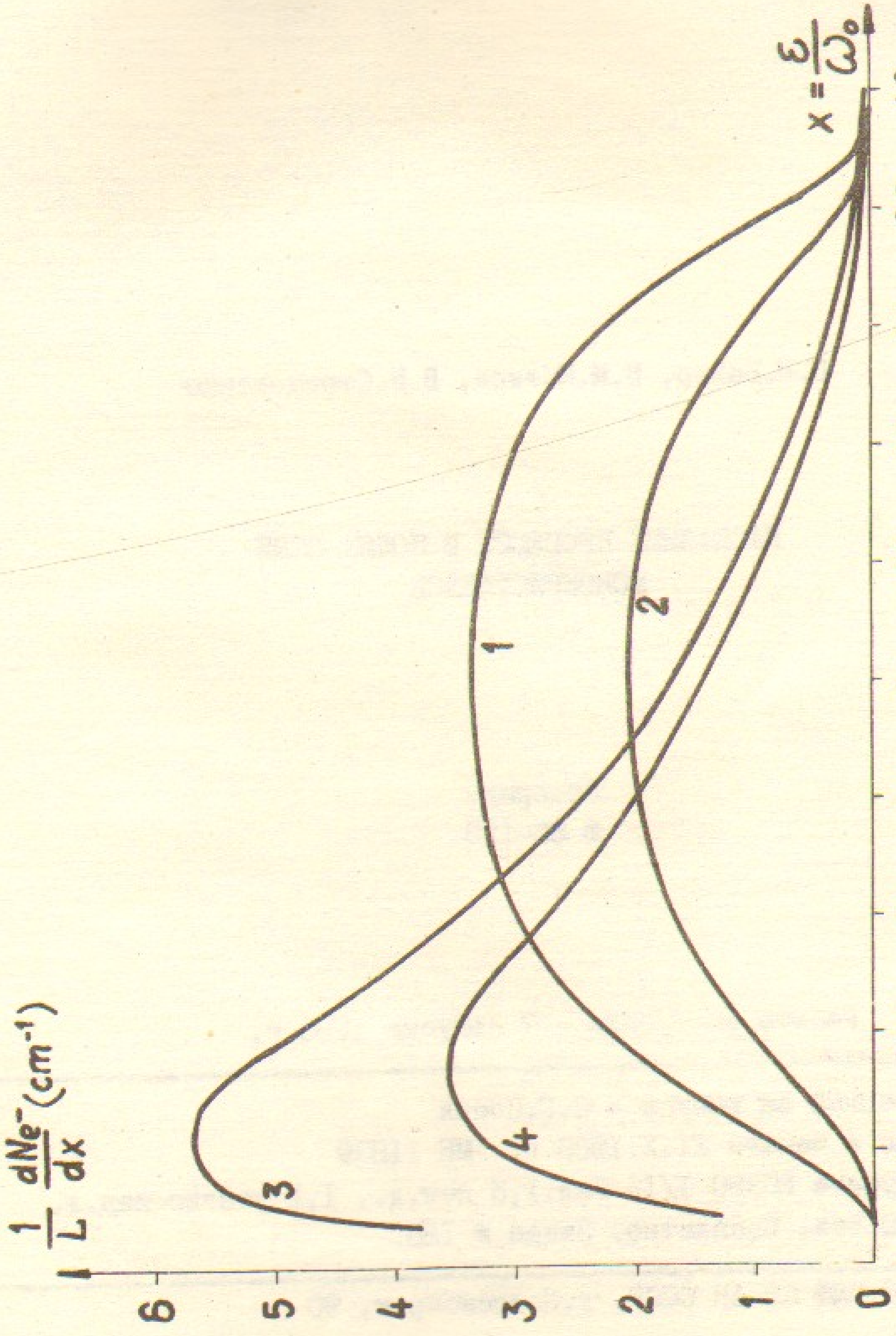
1/L dNe⁻/dx (cm⁻¹)
x = ε / ω₀
0
1
2
3
4
5
6
0.1
0.2
0.3
0.4
0.5
0.6
0.7
0.8
0.9
1.0
1
2
3
4

Fig.6

В.Н.Байер, В.М.Катков, В.М.Страховенко

КАСКАДНЫЕ ПРОЦЕССЫ В ПОЛЯХ ОСЕЙ
МОНОКРИСТАЛЛОВ

Препринт
№ 86-128

Работа поступила - 7 августа 1986 г.

Ответственный за выпуск - С.Г.Попов
Подписано к печати 21.X.1986 г. МН 11839
Формат бумаги 60x90 1/16 Усл.1,5 печ.л., 1,2 учетно-изд.л.
Тираж 250 экз. Бесплатно. Заказ № 128.

Ротапринт ИЯФ СО АН СССР, г.Новосибирск, 90